Advanced Ceramics Progress: Vol. ?, No. ?, (Season 202?) ??-??

Materials and Energy Research Center
MERC

Contents lists available at ACERP

Advanced Ceramics Progress

Journal Homepage: www.acerp.ir

Original Research Article

Construction of 0D/3D $ZnWO_4$-MoS_2 heterojunction with enhanced charge carrier separation for decomposition of organic pollutants under visible light irradiation

M.Farhadian*, M.R Akbarpour
Department of Materials Engineering, Faculty of Engineering , University of Maragheh, Maragheh, East Azerbayjan, Iran

* Corresponding Author Email: m.farhadian@maragheh.ac.ir (M. Farhadian)
URL: http://www.acerp.ir/article_90833.html

ARTICLE INFO

Article History:

Received ? Month 202?
Received in revised form ? Month 202?
Accepted ? Month 202?

Keywords:
MoS_2
$ZnWO_4$
Photocatalyst
Heterojunction

ABSTRACT

In this work, 0D/3D $ZnWO_4$-MoS_2 heterojunction was prepared through a two-step hydrothermal procedure and applied for degradation of MB dye from aqeous solution under visible light irradiation. XRD and FESEM analyses were conducted to conform the sucussful incorporation of $ZnWO_4$ nanoparticles over flowerlike MoS_2 structure. Based on the obtained results, heterojunction with 30% wt. of $ZnWO_4$ revealed the best photocatalytic performance compared to the other heterojunction samples. This improvement is mainly ascribed to the p-n heterojunction effect in which the photoinduced electrons and holes could be effectevly separated on the different semiconductors and facilitate the formation of radical active species, resulting in efficient enhancement of photocatalytic performance. Brsides, the results obtained from DRS analysis confirmed that visible light absorption of the heterojunction samples is decreased as the $ZnWO_4$ content exceed 30% wt. which is corresponded to the shielding effect of UV-responsive $ZnWO_4$ component. Hydroxyle radicals was determined as the main active species responsible for photodecomposition of MB.

1. INTRODUCTION

MoS_2 is a two-dimensional (2D) semiconductor material that has gained significant attention for its unique properties as a promising photocatalyst [1,2]. As a photocatalyst, MoS_2 can absorb visible light energy to promote chemical reactions, making it a potential solution for energy conversion and environmental remediation. MoS_2 exhibits excellent catalytic activity due to its high surface area, strong adsorption ability, and tunable bandgap [3–5]. Additionally, its layered structure and strong interlayer interactions result in efficient charge separation and transfer [6]. MoS_2 based photocatalysts have been studied for their applications in hydrogen evolution, water splitting, and degradation of organic pollutants [7]. Further research on MoS_2 as a photocatalyst may lead to the development of more efficient and sustainable technologies for various industrial and environmental applications [8]. Although

Please cite this article as: Farhadian, M, "Construction of 0D/3D $ZnWO_4$-MoS_2 heterojunction with enhanced charge carrier separation for decomposition of organic pollutants under solar light irradiation", ***Advanced Ceramics Progress***, Vol. ?, No. ?, (202?), ??-??.

MoS_2 has shown great potential as a photocatalyst, there are still some limitations that need to be addressed. Some of the notable limitations of MoS_2 as a photocatalyst include poor charge carrier mobility, limited light absorption and chemical insatbility [9].

As an n-type semiconductor, $ZnWO_4$ has the ability to utilize ultra viollent (UV) light energy to promote chemical reactions and degrade pollutants [10–12]. Its unique properties include high surface area, stability under harsh conditions, and efficient charge separation, which contributes to its high photocatalytic activity [13]. The combination of $ZnWO_4$ with MoS_2 semiconductors can broaden the absorption spectrum, thereby increasing the utilization of solar energy. In additiom, the $ZnWO_4/MoS_2$ heterojunction can promote charge separation, leading to more efficient electron-hole pair generation. This is because $ZnWO_4$ has a higher conduction band position than MoS_2, which facilitates the transfer of electrons from MoS_2 to $ZnWO_4$. The combination of $ZnWO_4$ and MoS_2 can improve the stability and durability of the photocatalyst. $ZnWO_4$ has good chemical stability and can protect MoS_2 from oxidation or corrosion under harsh reaction conditions [14]. Overall, the use of $ZnWO_4$ as a co-catalyst with MoS_2 can lead to improved photocatalytic performance, enhanced charge separation and transfer, and increased stability and durability.

In this study, 0D $ZnWO_4$ nanoparticles was loaded on 3D flowerlike MoS_2 microspheres and applied for decomposition of Methylen blue (MB) dye from aqeous solution through simple hydrothermal method. The pure and hybrid photocatalysts were characterized and their chemical, structural and optical features were studied.

2. MATERIALS AND METHODS

In this study $(NH_4)_6Mo_7O_{27}$, CH_4N_2S, $Na_2WO_4.2H_2O$, $Zn(NO_3)_2{\cdot}6(H_2O)$, ammonia solution (25%) and ethanol were purchased from Merck (Germany) and used without further purification.

The flower-like MoS_2 microspheres were synthesized by a one-step hydrothermal reaction using hexaammonium heptamolybdate tetrahydrate and thiourea as starting materials. In a typical synthesis, 1.24 g of hexaammonium heptamolybdate tetrahydrate and 2.28 g of thiourea were dissolved in 36 ml deionized water under vigorous stirring for 30 min to form a homogeneous solution. The solution was then transferred into a 50 ml Teflon-lined stainless steel autoclave and sealed tightly, heated at 220 ºC for 6 h and then naturally cooled down to room temperature. Black precipitates were collected by centrifugation and washed with distilled water and absolute ethanol for several times, and finally dried in vacuum at 60 °C for 24 h.

To prepare $ZnWO_4/MoS_2$ heterojunction with various weight ratio of $ZnWO_4$ content, $Zn(NO_3)_2.6H_2O$, $Na_2WO_4.2H_2O$ and CTAB were dissolved in the mixed solution of DMF (40 ml)/H_2O (10 ml). Then, 0.4 g MoS_2 was added to the clear solution and ultrasonically treated for 1 h until a homogeneous mixture was obtained. It was then transformed to the teflon-lined stainless steel autoclave and heat treated at 180 ºC for 12 h. The final products was filtered, collected, washed 3 times with ethanol and deionized water, and then dried in vaccum oven at 80 ºC for 12 h. The $ZnWO_4/MoS_2$ nanocomposites were denoted as 10ZM, 20ZM, 30ZM, 40ZM, in which the number represnts the weight percent of loaded $ZnWO_4$ nanopartiles on the surface of MoS_2.

3. RESULTS AND DISCUSSION

3.1. FE-SEM images

Figure 1 represents SEM images of MoS_2 flower-like microspheres and $ZnWO_4/MoS_2$ heterojuntion sample with 30 wt.% $ZnWO_4$ content (M30Z). From Figures 1a and 1b, hierarchical MoS_2 flowerlikes with approximately 1 µm in diameter are formed. In addition, $ZnWO_4$ nanoparticles with diameter of around 20 nm are homogeneously integrated among the MoS_2 layers as is clear in Figures 1c and 1d. As it could be obsorved, the MoS_2 microflowers retained thier original shapes after combination with $ZnWO_4$ nanoparticles, representing excellent stability of prepared MoS_2 hierarchical microstructures.

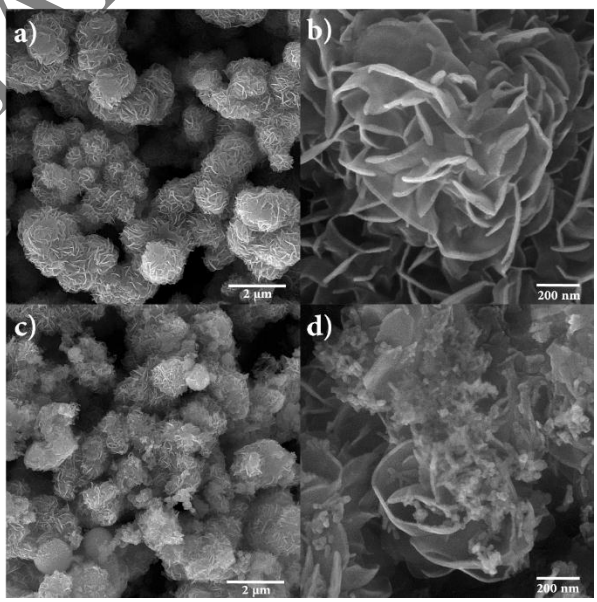

Figure 1. FESEM images of (a, b) MoS_2 microsphere and (c, d) $ZnWO_4/MoS_2$ heterojunction

3.2. XRD

XRD analysis was conducted to study the phase structure of the prepared samples. As seen in Figure. 2, the peaks at 2θ=14.5° (002), 34.2° (100), 39.0° (103), 49.5° (105) and 59.0° (110), can be asgined to hexagonal structure of MoS_2 (JPCDS No.00.037-1492). The peaks obsorved in the XRD pattern of pure $ZnWO_4$ could be attributed to its monoclinic phase (JPCDS No.00.015-0774). Further, the asgined peaks of $ZnWO_4$ were

appeared in the XRD pattern of the heterojunction samples, indicating the successful combination of $ZnWO_4$ nanoparticles with the MoS_2 structure. There exist no other peaks in the XRD patterns of heterojunction samples. This reveals that the composite samples with no other impurities are formed.

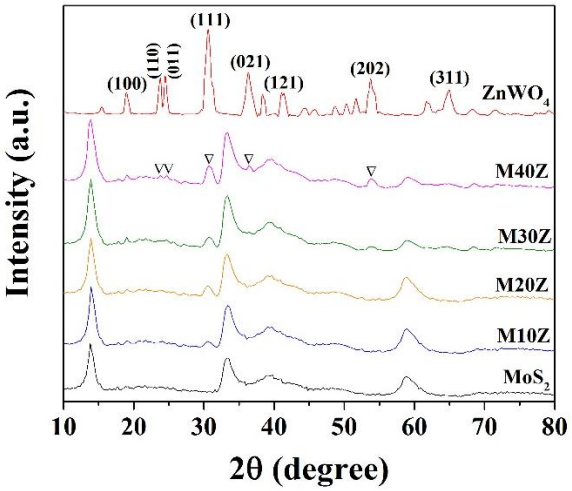

Figure 2. XRD patterns of the pure and heterojunction samples.

3.3 Optical properties

The optical properties of the prepared samples were measured by diffuse reflectance spectroscopy (DRS). As seen in Figure. 3, compared with pure MoS_2, the optical absorption edge of the heterojunction samples was shifted to the shorter wavelengths as $ZnWO_4$ content increased which is attributed to the larger band gap of $ZnWO_4$, indicating the construction of heterojunction at the interface of MoS_2 and $ZnWO_4$. The energy band gap (E_g) of the samples was calculated using the Kubelka-Munk equation $(\alpha h\upsilon)^n = A(h\upsilon - Eg)$, and the results represnted in Figure. 4. Accordingly, Eg of heterojunction samples was increased with icreasing the $ZnWO_4$ content compared to prinstine MoS_2. The presnece of both MoS_2 with narrow band gap and $ZnWO_4$ as a UV-responsive semiconductor benefits broader light absorption and heterojunction effect, which ultimately improve the photocatalytic performance.

3.4 Photocatalytic activity

Photocatalytic performance of the samples was evaluated through photodecomposition of MB from aqeous solution under visible light irradiation. The obtained results are shown in Figure 5. As is clear, MoS_2 revealed poor photocatalytic activity which is corresponded to the fast recombination rate of the electron-hole pairs, resulting from its narrow band gap. However, as $ZnWO_4$ is loaded on the surface of MoS_2 struture, the photodegradation activity is enhanced. This improvment is related to the heterojunction effect in which the produced electrons and holes in MoS_2 could effectively separaetd and then lifespan of the charge carriers is increased, facilitating the formation of active species. As seen, photocatalytic decomposition of MB is enhanced up to 30% wt. content of $ZnWO_4$ and then decreased. Indeed, $ZnWO_4$ component is not able to absorb visible light sepctrum due to its larger band gap. It seems that the higher ZWO_4 nanoparticles loading could cover the optical active sites of the MoS_2 hierarchical and decrease the visible light absorption, as could be seen in Figure 3, resulting in the photocatalytic performace of the M40Z heterojunction sample is decreased. To evaluate the stability of the optimum sample (M30Z), recycling experiments were conducted and shown in Figure 6. The results revealed that the photocatalytic degradation percentage of M30Z sample only decreased approximately 5%, showing good chemical stability.

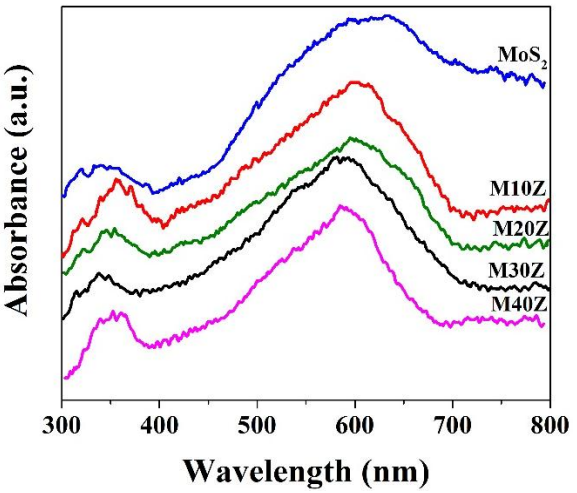

Figure 3. DRS plots of pure MoS_2 and prepared heterojunctions.

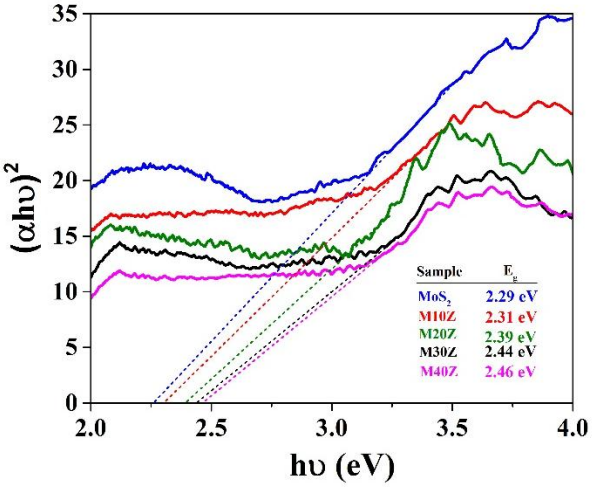

Figure 4. Tauc Plots of pure MoS_2 and prepared heterojunctions.

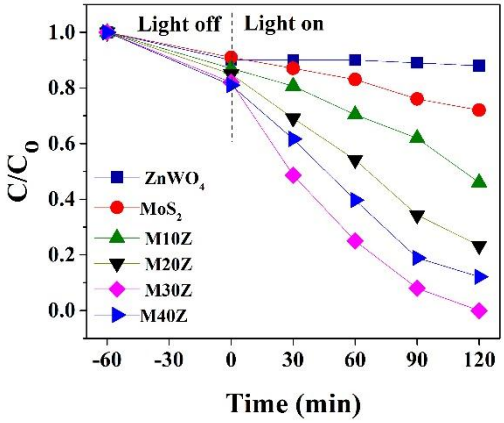

Figure 5. Photocatalytic decomposition of MB from aqeous solution over prepared pure and heterojunction samples under visible light irradiation.

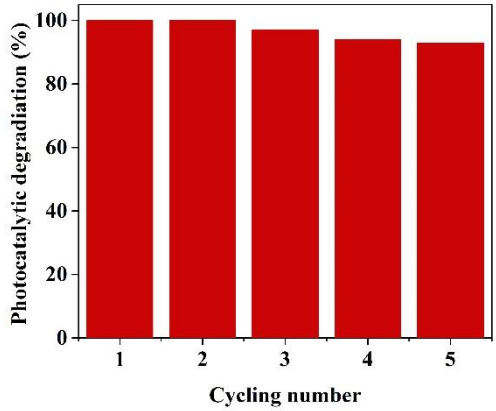

Figure 6. Recycling evaluation of M30Z sample toward MB decomposition under visible light irradiation.

3.5 Photocatalytic mechanism

To study the photocatalytic mechanism of the prepared heterojunction, radical trapping experiments were conducted to determine the active species responsible for the photocatalytic degradation of MB. For this, triethanolamine (TEA), benzoquinone (BQ), isopropyl alcohol (IPA) as scavengers of holes, superoxide radicals and hydroxide radicals, respectively, were separately added. As shown in Figure 7, the photodegradation of MB was slightly decreased in the presence of BQ, indicating that superoxide radicals evealed no significant role over photocatalytic decomposition of MB. In addition, the significant reduction of photocatlytic perfomance in the presence of IPA denoted that hydroxyle radicals are the main species for photodecomposition of MB. In addition, the photoinduced holes also involved for photodegradation of MB.

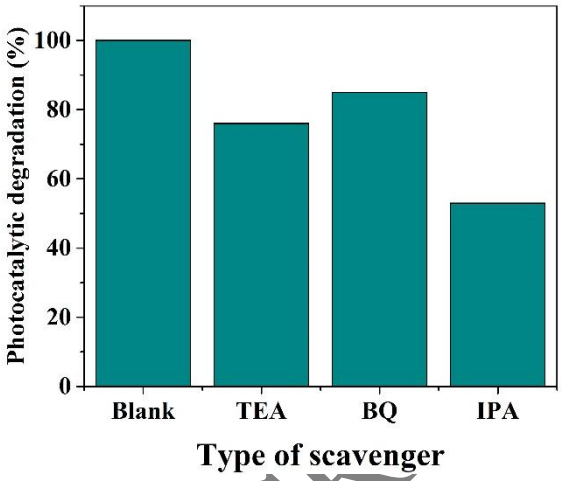

Figure 7. Photocatalytic degradation of MB in the presence of verious scavengers.

4. CONCLUSION

In summary, hierarchical $ZnWO_4$-MoS_2 heterojunction samples with different $ZnWO_4$ content were successfully prepared by a simple two-step hydrothermal method, and served toward photocatalytic degradation of MB dye from aqueous solutions under visible light irradiation. Based on the obtained results, $ZnWO_4$-MoS_2 heterojunction with 30 mol. % content of $ZnWO_4$ revealed 8.33 times enhancement after 120 min irradiation compared to pure MoS_2. This improvement is mainly attributed to the heterojunction effect during which photoinduced electrons and holes over MoS_2 could effectively separated and easily participate for the radical species production. Further, recycling experimets showed that the fabricated $ZnWO_4$-MoS_2 revealed only around 5% reduction in photodegradation of MB which represents that sufficient bondings are formed at their interface. Further, the results indicated that hydroxyle radical along with photoinduced holes are the main species toward photocatalytic degradation of MB. The obtained results verify that the prepared $ZnWO_4$-MoS_2 heterojunction could be a promising visible-light-acivated photocatalyst for efficient degradation of dye contaminants from wastewater.

REFERENCES

[1] W. Li, L. Wang, Q. Zhang, Z. Chen, X. Deng, C. Feng, L. Xu, M. Sun, Fabrication of an ultrathin 2D/2D C3N4/MoS2 heterojunction photocatalyst with enhanced photocatalytic performance, Journal of Alloys and Compounds. 808 (2019) 151681.

[2] N.R. Khalid, M.R. Kamal, M.B. Tahir, M. Rafique, N.A. Niaz, Y. Ali, M. Alzaid, H. Alrobei, S. Muhammad, Fabrication of direct Z-scheme MoO3/N–MoS2 photocatalyst for synergistically enhanced H2 production, International Journal of Hydrogen Energy. 46 (2021) 39822–39829.

[3] Z. Li, X. Meng, Z. Zhang, Recent development on MoS2-based photocatalysis: A review, Journal of Photochemistry

and Photobiology C: Photochemistry Reviews. 35 (2018) 39–55.

[4] J. Sun, X. Li, W. Guo, M. Zhao, X. Fan, Y. Dong, C. Xu, J. Deng, Y. Fu, Synthesis methods of two-dimensional MoS2: A brief review, Crystals. 7 (2017) 198.

[5] Z. Liang, R. Shen, Y.H. Ng, P. Zhang, Q. Xiang, X. Li, A review on 2D MoS2 cocatalysts in photocatalytic H2 production, Journal of Materials Science & Technology. 56 (2020) 89–121.

[6] S. Huang, C. Chen, H. Tsai, J. Shaya, C. Lu, Photocatalytic degradation of thiobencarb by a visible light-driven MoS2 photocatalyst, Separation and Purification Technology. 197 (2018) 147–155.

[7] Y.-J. Yuan, P. Wang, Z. Li, Y. Wu, W. Bai, Y. Su, J. Guan, S. Wu, J. Zhong, Z.-T. Yu, The role of bandgap and interface in enhancing photocatalytic H2 generation activity of 2D-2D black phosphorus/MoS2 photocatalyst, Applied Catalysis B: Environmental. 242 (2019) 1–8.

[8] Y. Yuan, R. Guo, L. Hong, X. Ji, Z. Li, Z. Lin, W. Pan, Recent advances and perspectives of MoS2-based materials for photocatalytic dyes degradation: a review, Colloids and Surfaces A: Physicochemical and Engineering Aspects. 611 (2021) 125836.

[9] E. Cui, G. Yu, H. Huang, Z. Li, Current advances in MoS2/semiconductor heterojunction with enhanced photocatalytic activity, Current Opinion in Green and Sustainable Chemistry. 6 (2017) 42–47.

[10] H.L. Abubakar, J.O. Tijani, S.A. Abdulkareem, A. Mann, S. Mustapha, A review on the applications of zinc tungstate (ZnWO4) photocatalyst for wastewater treatment, Heliyon. (2022).

[11] H. Fu, J. Lin, L. Zhang, Y. Zhu, Photocatalytic activities of a novel ZnWO4 catalyst prepared by a hydrothermal process, Applied Catalysis A: General. 306 (2006) 58–67.

[12] A.O.C. Andrade, L.H. da Silveira Lacerda, M.M.L. Júnior, S.K. Sharma, M.E.H.M. da Costa, O.C. Alves, E.C.S. Santos, C.C. dos Santos, A.S. de Menezes, M.A. San-Miguel, Enhanced photocatalytic activity of BiOBr/ZnWO4 heterojunction: A combined experimental and DFT-based theoretical approach, Optical Materials. 138 (2023) 113701.

[13] V. Rathi, A. Panneerselvam, R. Sathiyapriya, Graphitic carbon nitride (g-C3N4) decorated ZnWO4 heterojunctions architecture synthesis, characterization and photocatalytic activity evaluation, Diamond and Related Materials. 108 (2020) 107981.

[14] R. Atla, T.H. Oh, Solar light-driven 2D MoS2 nanoflake-supported 1D ZnWO4 nanorod heterostructure: Efficient separation of charge carriers for removing toxic organic pollutants, Journal of Environmental Chemical Engineering. 9 (2021) 106427.